[6] G. Krafft, private communication.

accommodate variations in injector bunch length and injector and linac RF phase.

Figure 6: Longitudinal phase space at wiggler for constant energy in the presence of 1^o variations in linac phase. Injection and linac parameters are as in Figure 3.

Acknowledgments

The first author would like to thank Drs. J. Bisognano, L. Harwood, and G. Krafft for useful discussions during the preparation of this note. We note that many bunch manipulations. In addition, we thank Dr. G. Neil for a careful reading of, and useful comments on, a draft version of this note.

References

[1] Laser Processing Consortium, “Free-Electron Lasers for Industry”, April 1995 (includes conceptual design report for an SRF-based FEL driver).

[2] L. Wells, Notes from CEBAF Accelerator Division FEL Retreat, Kingsmill Conference Center, Williamsburg, VA, 6-10 February 1995 (unpublished).

[3] C. Leemann (unpublished).

[4] *ibid.*; Laser Processing Consortium, *op. cit.*; D. Neuffer (unpublished); A. S. Sokolov and N. A. Vinokurov, N. I. M., A341, pp. 398-401, 1994.

[5] Laser Processing Consortium, *op. cit*. We note that the demonstration driver is multipass and has some optimization of the momentum spread from pass to pass; the beam therefore rides on crest through the first pass in linac and 20^o off-crest during the second. The net effect is equivalent, at the wiggler, to riding off crest by 10^o throughout the acceleration cycle. In addition, small (order of 20%) deviations in M_{56} and T_{566} from scaling law values are imposed in the detailed driver design so as to compensate wake field effects, which were ignored in the above treatments.

tional experience with the CEBAF injector demonstrates that injection energy is readily regulated to better than the 10^{-3} level, even without the use of spectrometer-based feed-back. Assuming some bending in the injection line, even better control of injection energy can be expected by feedback on injector cavity gradients. Similarly, CEBAF injector experience indicates that injection bunch lengths can be quickly measured and set to high precision, and then held for periods of several hours. We therefore do not expect injector parametric goals to be difficult to achieve during initial driver operations.

Operational experience with the CEBAF injector and linac also indicate parameters associated with the driver accelerator can be readily managed during initial turn-on. Energy gain through an SRF linac can be regulated to the 10^{-4} level or better through the use of spectrometer-based feedback to cavity gradients; E^{FEL} stability should therefore be operationally tractable. We note that energy shifts in SRF systems typically are not due to variations in RF voltage or gradient, but are rather due to shifts in RF phase. Such energy variations are easily compensated by a change in gradient; the issue of phase variation and correction is taken up below. M_{56} has been measured and set with high precision in the CEBAF transport system, and T_{566} can readily be managed in the same fashion. In fact, manipulations of quantities dynamically equivalent to M_{56} and T_{566} is routinely performed in the CEBAF injector during bunch length measurements and adjustments; bunch compression and energy spread management manipulations completely analogous to those described here have been operationally implemented in the CEBAF injector for some time [6].

The remaining free parameter is the linac phase offset. Experience at CEBAF indicates that significant phase drifts (of a few degrees) within the injector and linac can occur on a time scale of hours. These variations affect both the final energy and momentum spread of the beam, and are therefore of concern for driver operations. As noted above, the central energy of the beam is readily stabilized with an “energy lock” system, but phase drifts, over the course of hours, can result in the generation of large energy spreads. During FEL operation, this can lead to loss of gain due to excessive energy spread and bunch lengthening (drop of peak current).

To determine the impact of phase drifts in the driver under consideration here, we have used the above relations to evaluate numerically the beam phase space at the wiggler when a long injected bunch is accelerated at various phases. The base parameters are the same as in Figure 3; a nominal phase offset of 10^{o} was used to establish the final energy and magnetic compression parameters for the system. The phase offset was then varied in 0.5^{o} increments, and the RF voltage adjusted to keep the bunch central energy constant. As indicated by the phase space images in Figure 6, the system is tolerant to phase variations on the order of one half degree. During normal operations the driver could therefore be run for a period of hours, and then an interruptive correction of injected bunch length, linac phase, and linac energy gain could be performed. This is the manner in which CEBAF linac operations

approach and confirmed by ray tracing have demonstrated that manageable longitudinal scenarios can be developed for up to several passes [4]. However, in systems studied to date, one or more of the lower energy passes has been constrained to transport extremely large momentum spreads (on the order of 10%), especially during energy recovery. This situation places severe demands on the magnetic lattice of these passes; higher order chromatic aberrations in both the transverse and longitudinal dimensions will generally cause severe distortion of the phase space and lead to unacceptable rates of beam loss.

Example - CEBAF Demonstration Driver

To illustrate the use of the above scaling laws, we apply them to a parameter set for the CEBAF FEL Demonstration Project [1] that was developed during discussions in February 1995 [2]. The base parameter list is as follows.

- injected bunch length - 4 p-sec (1.2 mm)
- injection energy - 10 MeV
- FEL electron beam energy 200 MeV
- maximum relative energy spread at wiggler - 0.7%
- bunch length at wiggler - 0.2 p-sec (60 microns)

We first determine the RF wavelength; using the above result we find it can have a lower limit of approximately 10 cm. We therefore chose the canonical CEBAF value of 20 cm. Given this, and the above scaling laws, we find the linac energy gain is to be 190 MeV, the phase offset should be about 10^{o}, M_{56} should be 17 cm, and T_{566} should be 2.4 m. These values are all quite similar to the results quoted in the design report for the Demonstration FEL [5].

Operational Considerations

Successful operation of the FEL/driver under consideration will require either appropriate levels of regulation of all critical parameters or design features reducing sensitivity to errors in these parameters. The above discussion relating the key parameters of the system leads naturally to consideration of this issues; in this section, we therefore sketch an operational scenario/error management scheme for an FEL driver. We note that the following discussion holds only for initial turn-on at modest (order of 100 μA) currents; high (order 1 to 10 mA) current operation is an as yet unexplored region, in which effects such as space charge, wake fields, and beam loading of the RF drive system (all ignored above) could be quite important.

The principle parameters to be maintained are the beam energy at the wiggler, E^{FEL}, the energy spread at the wiggler, ΔE^{FEL}, and the peak current/bunch length at the wiggler, specified by L_{bunch}^{FEL}. These must be controlled by appropriate regulation of the other parameters discussed above. Starting from the injector, we note that opera-

and T_{566} in the arc downstream of the wiggler.

$$M_{56}^{down} = M_{56}^{up}$$

$$T_{566}^{down} = T_{566}^{up}$$

These relations presuppose the stated acceleration scenario - namely, that the beam rides off-crest through a linac on one pass up and one pass down. The situation is idealized, inasmuch as effects of third and higher order have been ignored. Just as these effects give rise to nonlinear bunch lengthening at the wiggler during acceleration, we expect them to lead to nonlinear growth in momentum spread at the dump during deceleration. The magnitude of this effect can be evaluated in the manner described above in the treatment of third order bunch lengthening.

Application to Multipass Machine

The single pass driver model may be extended to describe multi-pass machines in either of two ways. The most simple extension is to impose the design requirement that $M_{56} = 0$ and $T_{566} = 0$ and that the beam path length be an integral multiple of the RF wavelength for all but the highest energy arc. In this case, the multi-pass longitudinal dynamics of the acceleration and deceleration cycles are the same as in the case of a single long linac. This approach does not in general provide the smallest achievable momentum spreads in each of the lower energy arcs during the acceleration cycle, and can therefore lead to problems with momentum acceptances.

The second extension of the model is to simply concatenate the above transformations for each pass through the driver linac. This allows optimization of momentum spreads through the acceleration and deceleration cycle, but is done at the cost of introducing numerous new parameters, most particularly the choice of M_{56} and T_{566} in each arc, the momentum spread and bunch length in each arc, and the beam path length through each arc (which dictates the beam RF phase on the next pass through the linac). This process, though well defined, is tractable to high order only numerically for machines with more than a small number of passes.

Analytically, one may, however, treat the *linear* portion of the motion in a many-pass machine using a “thin-lens - drift” model [3]. In this approach, a pass through the linac and around an arc is treated as a longitudinal lens (the linac) followed by a longitudinal drift (the arc, with M_{56} as the drift length). Periodicity conditions can then be applied to the system and it may be described in terms of matched betatron functions and tunes. Analysis of momentum spreads and bunch lengths throughout the system can then be performed by evaluating the usual “spot size” formulae involving the longitudinal emittance and beta functions.

Numerical and analytical studies of many-pass systems based on this linear

Application to Energy Recovery Cycle

The treatment outlined above may be applied to the energy recovery cycle as well. Conceptually, a short, large (several percent) energy spread bunch leaves the wiggler and is transported through an arc in which a nonzero M_{56} and T_{566} "slew" it. The bunch is then sent though the linac out of phase with the RF, so that it decelerates while energy compressing; the resulting bunch at the end of the energy recovery cycle is long and has small momentum spread. The process is depicted schematically in Figure 5.

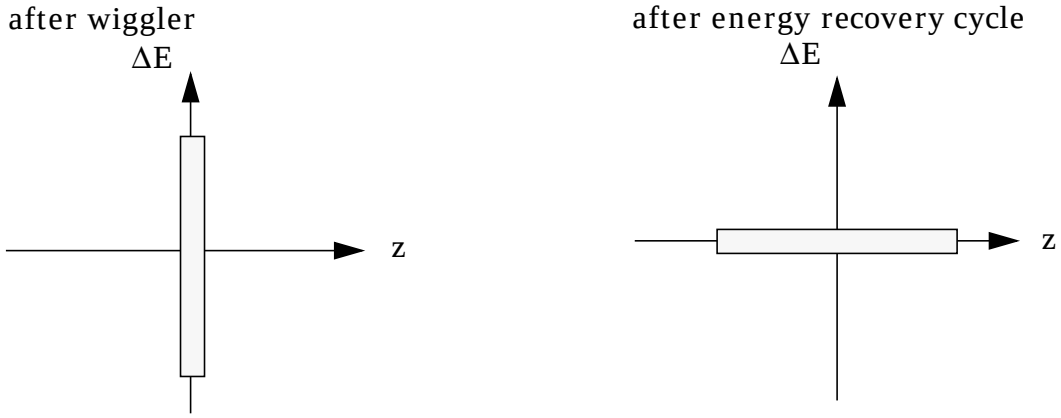

Figure 5: Idealized longitudinal phase space management during energy recovery.

The description of the energy recovery cycle corresponds exactly to that of the acceleration cycle, in reverse order. Thus, scaling laws relating, for example, the energy spread after lasing to the bunch length following energy recovery and the phase offset during deceleration, may be derived. For the specific example given, we find the following expression holds.

$$\sin\phi_0 \approx \frac{1}{2\pi} \frac{(\Delta E^{FELoutput}/E^{FEL})}{(L_{bunch}^{recovered}/\lambda)}$$

This is a consequence of the fact that the phase offset during the deceleration cycle is the same (modulo 180^o) as during the acceleration cycle, because the final central energy must be essentially the same as the injected energy. Equating the two expressions for $\sin\phi_0$ gives the following relation amongst the energy spreads and the bunch lengths,

$$\frac{\Delta E^{FELoutput}}{\Delta E^{FEL}} = \frac{L_{bunch}^{recovered}}{L_{bunch}^{inj}}$$

and extensions of the arguments given above lead to the following conditions on M_{56}

$$\sin\phi_0 \approx \frac{1}{2\pi} \frac{(\Delta E^{FEL}/E^{FEL})}{(L^{inj}_{bunch}/\lambda)}$$

Given the phase offset, the wavelength, and the FEL energy spread, key lattice parameters are determined; these may be estimated using simple scaling relations.

$$M_{56} \approx \frac{L^{inj}_{bunch}}{(\Delta E^{FEL}/E^{FEL})}$$

$$T_{566} \approx \frac{2\pi^2}{\lambda^2} M_{56}^3$$

These relations call out the parameters and assumptions of interest in the design process. Key parameters are the injected bunch length, the RF wavelength, the FEL energy and energy spread. Key assumptions are that the beam is injected with relatively small momentum spread (such as $\delta p/p \sim 10^{-3}$), that the bunch is kept long during the acceleration cycle, and that bunch compression, to a achieve high peak current in the FEL, is done immediately before the wiggler. The relationships amongst these parameters are schematically depicted in Figure 4.

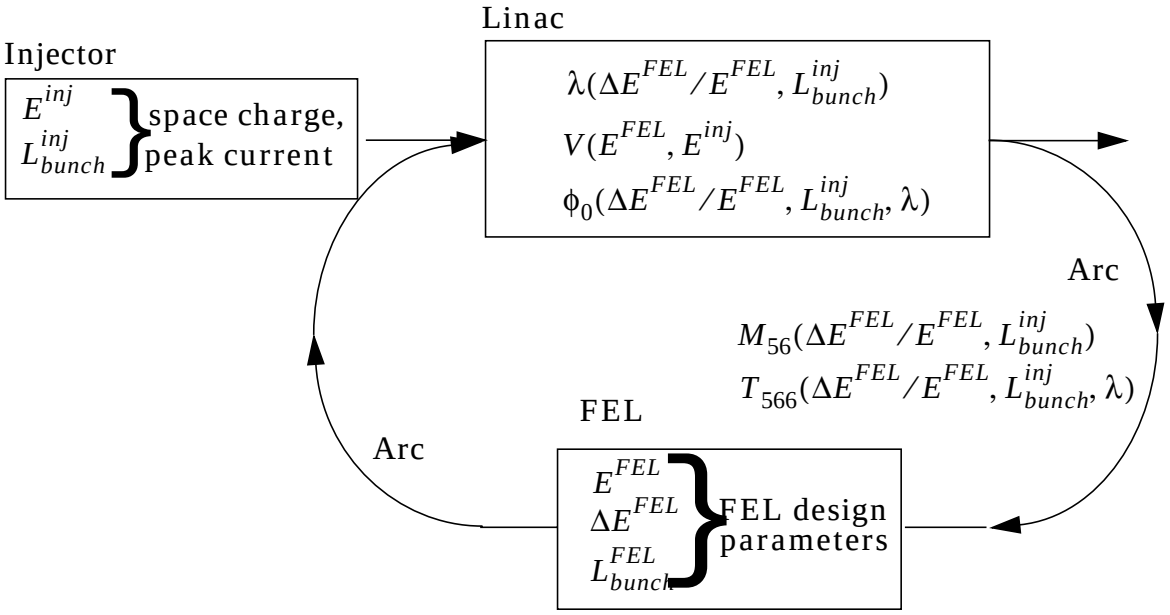

Figure 4: Schematic relationship amongst FEL, injector and driver parameters.

FEL energy spread, and the RF wavelength.

$$\frac{L_{bunch}^{FEL}}{2} = \left(\frac{8\pi^4 (L_{bunch}^{inj})^2}{\delta_{FEL}^2} \frac{1}{\lambda^4} - \frac{4\pi^2}{3} \frac{1}{\lambda^2} \right) \left(\frac{L_{bunch}^{inj}}{2} \right)^3$$

This can be rearranged into a quartic equation for $(L_{bunch}^{inj}/\lambda)$

$$\left(\frac{L_{bunch}^{inj}}{\lambda} \right)^4 - \frac{\delta_{FEL}^2}{6\pi^2} \left(\frac{L_{bunch}^{inj}}{\lambda} \right)^2 - \frac{\delta_{FEL}^2}{2\pi^4} \left(\frac{L_{bunch}^{FEL}}{L_{bunch}^{inj}} \right) = 0$$

with the solution given below.

$$\left(\frac{L_{bunch}^{inj}}{\lambda} \right) = \sqrt{\frac{1}{2} \frac{\delta_{FEL}^2}{6\pi^2} \pm \sqrt{\frac{1}{4} \frac{\delta_{FEL}^4}{36\pi^4} + \frac{\delta_{FEL}^2}{2\pi^4} \left(\frac{L_{bunch}^{FEL}}{L_{bunch}^{inj}} \right)}}$$

The latter relation specifies, for fixed injector bunch length L_{bunch}^{inj}, bunch length at the wiggler L_{bunch}^{FEL}, and energy spread δ_{FEL}, a lower limit on the RF wavelength λ.

Summary

We now summarize the relations amongst the parameters of the system. The injection energy E^{inj} is set by cost optimization and a desire to avoid problems with space charge. The injector bunch length L_{bunch}^{inj} is set to relatively long values to avoid high peak currents and reduce space charge effects. The beam energy at the wiggler, E^{FEL}, is set by FEL needs, as is the maximum allowable energy spread at the wiggler. The bunch length must be short at the wiggler to produce a high peak current and is therefore limited to some value L_{bunch}^{FEL}. It is, however, desirable to keep the bunch long through the acceleration process to limit peak currents in the accelerator. This implies compression should be done at the end of the acceleration cycle.

These parametric and design choices dictate the parameters for the driver accelerator. The RF wavelength λ is a key linac parameter and has a lower limit given by the injected bunch length, the bunch length limit at the wiggler, and the FEL momentum spread limit. This wavelength limit is driven by the need to avoid introducing third-order distortion-induced bunch lengthening at the wiggler. Other variables are fixed by injector and FEL requirements. The choice of injection and FEL energy determines the required linac energy gain V; the limit on ΔE^{FEL} and the injected bunch length then dictate the RF phase offset, which is given by the following scaling relation.

(This ignores the third order contribution from W_{5666} which, we stated above, is assumed to be set to zero in the lattice design). If this is expanded through third order, and the values for M_{56} and T_{566} derived above inserted, we obtain the following expression for the “third-order remnant” displacement at the wiggler.

$$\bar{z}_{R3} = \frac{2\pi^2}{\lambda^2}\left(\frac{1}{(\sin\phi_0)^2} - \frac{2}{3}\right)z^3$$

Recall that (under assumptions designed to limit this very third order effect) the phase angle is set by the energy spread at the FEL, the injected bunch length, and the RF wavelength (we consider “Case 1”).

$$\sin\phi_0 \approx \frac{1}{2\pi}\,\frac{(\Delta E^{FEL}/E^{FEL})}{(L^{inj}_{bunch}/\lambda)}$$

This indicates the final offset depends on the initial as follows.

$$\bar{z}_{R3} = \frac{2\pi^2}{\lambda^2}\left(\frac{4\pi^2}{\delta^2_{FEL}}\left(\frac{L^{inj}_{bunch}}{\lambda}\right)^2 - \frac{2}{3}\right)z^3$$

Here we have defined $\delta_{FEL} = \Delta E^{FEL}/E^{FEL}$; we note that the coefficient of z^3 blows up for small wavelength and vanishes for large wavelength. This would imply that longer is better (as indeed it is). If, however, we investigate the details (for example, by setting $\partial\bar{z}_{R3}/\partial\lambda = 0$ to search for any minima) we rapidly run into trouble, inasmuch as the coefficient $(1/(\sin\phi_0)^2 - 2/3)$ is positive definite, while the result of the optimization (a wavelength of about 1.9 m) would indicate that it is negative! We must either couple in this constraint in some fashion (it is lost because we have used a linear approximation for $\sin(2\pi L^{inj}_{bunch}/\lambda)$ in the expression for $\sin\phi_0$) or seek an alternative criterion. An alternative is clear - in order to maintain the peak current, the bunch length at the wiggler cannot be significantly degraded by this third order effect. We may therefore place an upper limit on $\bar{z}_{R3}$, and seek a (lower) limit on the RF wavelength that will allow us to satisfy this bunch length limit.

Given the total third order contribution must lie within the specified bunch length at the wiggler, we note that the point with displacement at the bunch half-length ($\bar{z} = L^{FEL}_{bunch}/2$) is the image of the head or tail of the bunch at injection ($z = L^{inj}_{bunch}/2$). By combining this information with the above results, we obtain an expression relating the tolerable bunch lengthening to the injected bunch length, the

of the waveform from a point offset from crest by the phase offset plus a half bunch length.

$$\Delta E^{FEL} = V\left[1 - \cos\left(|\phi_0| + \frac{\pi L_{bunch}^{FEL}}{\lambda}\right)\right]$$

Since the bunch length is assumed to be longer than the phase offset, and as the bunch length should be only fraction of the RF wavelength so as to avoid cubic and higher-order bunch lengthening at the wiggler, the phase offset must be small for the system to have reasonable performance. We may therefore expand and linearize the above relation to obtain the following expression (in which we have used the approximation $V \cong E^{FEL}$).

$$|\phi_0| \approx \frac{1}{\pi}\,\frac{(\Delta E^{FEL}/E^{FEL})}{(L_{bunch}^{inj}/\lambda)}$$

This is identical to the expression in case 1, save for a factor of 2; scaling expressions for M_{56} and T_{566} may therefore be obtained in an analogous fashion and have identical functional dependences (but with different weights) on the injected bunch length and relative energy spread at the wiggler. We note that Case 2 is less likely to arise than Case 1, inasmuch as even at a relatively high frequency such as 1.5 GHz, the injected bunch length is only a small fraction of the RF wavelength. The constraint that the phase offset be even smaller implies an unneccessarily tight tolerance on energy spread at the wiggler, and drives the required M_{56} and T_{566} to large values.

Third Order Effects and Constraints on the RF Wavelength. As noted above, we could in principle continue the expansion of longitudinal displacement at the wiggler to third (or higher) order and thereby establish constraints on the matrix element W_{5666}. As an alternative, we could correct the lattice contribution to the longitudinal displacement (design for $W_{5666} = 0$) and demand the remaining third order variation in displacement meet some different constraint. The remnant in question, which is due to higher order variations in the RF wave form coupling through the nonzero M_{56} and T_{566}, must not “significantly” lengthen the bunch at the wiggler (least the peak current fall to unacceptably low values), and can be controlled by the choice of RF wavelength. We can therefore develop a scaling law constraining the RF wavelength by demanding the third order contribution lie within the specified bunch length at the wiggler, L_{bunch}^{FEL}.

We proceed by recalling a longitudinal displacement z at the injector is imaged to a longitudinal displacement $\bar{z}$ at the wiggler as follows.

$$\bar{z}(z) = z - M_{56}\left(\frac{V}{E^{FEL}}\right)\left[\cos\left(\phi_0 - \frac{2\pi z}{\lambda}\right) - \cos\phi_0\right] - T_{566}\left(\frac{V}{E^{FEL}}\right)^2\left[\cos\left(\phi_0 - \frac{2\pi z}{\lambda}\right) - \cos\phi_0\right]^2$$

following relation specifying the phase, in which the assumption is made that injection energy is small compared to the linac energy gain (so that $V \cong E^{FEL}$).

$$\sin\phi_0 = \frac{1}{2\pi} \frac{(\Delta E^{FEL}/V)}{(L^{inj}_{bunch}/\lambda)} \approx \frac{1}{2\pi} \frac{(\Delta E^{FEL}/E^{FEL})}{(L^{inj}_{bunch}/\lambda)}$$

The above relation may be viewed as putting a limit on the phase offset; if ΔE^{FEL} is limited to a maximum value by FEL constraints, for a specific injected bunch length (which may be dictated by injector needs, such as limiting space charge effects) and linac energy gain (which is specified by the required final energy E^{FEL}), the above relation limits the maximum phase offset that can be used in slewing the energy for bunch compression purposes.

Given the phase offset, the compression parameters for the lattice follow. Inserting the result for $\sin\phi_0$ into the expression for M_{56} yields (with the identification of the FEL energy as $E^{FEL} = E^{inj} + V\cos\phi_0$) the following exact expression.

$$M_{56} = \frac{\lambda}{\pi}\left(\frac{E^{FEL}}{\Delta E^{FEL}}\right)\sin\left(\frac{\pi L^{inj}_{bunch}}{\lambda}\right) .$$

Under the bunch length assumptions outlined above, we may use the linearized expression for the phase offset to obtain the following simple scaling law for M_{56}.

$$M_{56} \approx \frac{L^{inj}_{bunch}}{(\Delta E^{FEL}/E^{FEL})}$$

Similar manipulations may be performed with the T_{566} expression. Noting that the phase offset is typically quite modest, so that $\cos\phi_0 \approx 1$, we may use the above result for phase offset and M_{56} in the exact expression for T_{566} to obtain the following scaling relation (in which we have again applied the approximation $V \cong E^{FEL}$).

$$T_{566} \approx \frac{2\pi^3}{\lambda^2} M_{56}^3$$

Case 2: Phase Offset Smaller Than Half-Length of Bunch. In this case, the bunch straddles crest (though asymmetrically, if the phase offset is nonzero, as it must be if M_{56} and T_{566} are to be finite), and the momentum offset is not monotonically varying as we move along the bunch. In this case, the energy spread is specified by the following expression, which gives the energy deviation of a point on the crest

In this treatment, it has been assumed that the energy “slew” required for magnetic compression has been imposed during the acceleration cycle and is taken out during the deceleration cycle; no separate, dedicated function RF system has been invoked for this purpose.

Scaling Relations

Having specified key lattice parameters entirely in terms of linac parameters, we now move to relate the linac parameters to the parameters of choice - namely, the injected bunch length and the energy spread at the wiggler. The connection in question is made through the relation for energy deviation:

$$\Delta\bar{E}(z) = V\left[\cos\left(\phi_0 - \frac{2\pi z}{\lambda}\right) - \cos\phi_0\right]$$

This expression leads directly to an expression for the final energy spread as a function of initial bunch length. There are two cases to be treated. The first occurs when the phase offset is greater than half the bunch length, so that the energy varies monotonically along the bunch. The second occurs when a portion of the bunch lies across the crest of the RF wave-form, and arises when the phase offset is less than half the bunch length. We treat each of these in turn.

Case 1: Phase Offset Greater Than Half-Length of Bunch. In this case,

$$\Delta E^{FEL} = \left|\Delta\bar{E}(z = L_{bunch}^{inj}/2) - \Delta\bar{E}(z = -L_{bunch}^{inj}/2)\right|$$

and using the above expression for $\Delta\bar{E}(z)$, we may derive an explicit expression for the energy spread, which is given below.

$$\Delta E^{FEL} = 2V\sin\phi_0\sin\left(\frac{\pi L_{bunch}^{inj}}{\lambda}\right)$$

This specifies the phase offset in terms of the injected bunch length as follows.

$$\sin\phi_0 = \frac{\Delta E^{FEL}}{2V\sin\left(\dfrac{\pi L_{bunch}^{inj}}{\lambda}\right)}$$

In most cases, we expect $L_{bunch}^{inj} \ll \lambda$; otherwise third and higher order terms in the RF waveform contribute significantly to the bunch length at the wiggler and it is difficult to perform the bunch compression. Consequently, we can linearize to obtain the

The centroid energy transforms as follows.

$$\bar{E}(z=0) = E^{inj} + V\cos\phi_0$$

As described above, this transformation must map a long, monoenergetic bunch into a zero length bunch of specified momentum spread. This can be accomplished through second order in z by appropriate choice of M_{56} and T_{566}. To obtain the required values, simply expand the displacement equation in z, and constrain it to vanish order-by-order in z. The first order constraint yields an expression for M_{56}, the quadratic constraint defines T_{566}.

$$M_{56} = \frac{\lambda}{2\pi}\frac{(E^{inj} + V\cos\phi_0)}{V}\frac{1}{\sin\phi_0}$$

$$T_{566} = \frac{\lambda}{4\pi}\left(\frac{E^{inj} + V\cos\phi_0}{V}\right)^2\frac{\cos\phi_0}{(\sin\phi_0)^3}$$

Using these relations, it is possible to compute the lattice properties required to compress the injected bunch, taking out both slope and curvature effects from the RF waveform. These properties are completely determined by injection energy, linac energy gain, RF phase offset and RF wavelength. Figure 3 presents an example of such a compression, in which a 4 p-sec monoenergetic bunch at 10 MeV is injected into a 200 MeV, 1.5 GHz linac 10^o off crest, and propagated through the linac and to a wiggler through an arc with M_{56} and T_{566} selected using the above expressions. Remnant curvature in the phase space is due entirely to third and higher order effects in the RF waveform. This can, in principle, be taken out by introduction of third order compensation via W_{5666}. We will discuss third order issues in more detail in the next section.

Figure 3: Longitudinal phase space evolution from 10 MeV injector through 200 MeV, 1.5 GHz linac and arc with M_{56} and T_{566} computed as detailed above.

The transform for the total centroid energy (at the z=0 point) is as follows. This total energy must equal the required FEL electron beam energy E^{FEL}.

$$\tilde{E}(z=0) = E^{inj} + V\cos\phi_0$$

The above equations fully specify the effect of the linac on the longitudinal phase space.

Arc Transform. The arc transform maps the phase space following the linac onto the phase space at the wiggler. It is as follows.

$$\bar{z}(\tilde{z}) = \tilde{z} - M_{56}\left(\frac{\Delta\tilde{E}}{\tilde{E}}\right) - T_{566}\left(\frac{\Delta\tilde{E}}{\tilde{E}}\right)^2$$

$$\Delta\bar{E}(\tilde{z}) = \Delta\tilde{E}$$

The centroid energy is given by the following expression (which simply states the energy is unchanged).

$$\bar{E}(\tilde{z}=0) = \tilde{E}(z=0)$$

The sign in the displacement equations is a consequence of use of DIMAD notation and the fact that longer path length ($\delta l > 0$) leads to a retardation of arrival time or phase relative to the bunch centroid, and thus corresponds to motion toward $z < 0$. The energy of the incoming beam is assumed to match the excitation point of the arc; failure to meet this condition causes a feed-down, in the displacement equation, of all higher order matrix elements (U_{5666}, W_{56666}, ...) resulting in a translation of the centroid position ($\bar{z}_{centroid}$ is no longer zero) and a shift, by amounts related to the energy error and the higher order terms, in the linear and quadratic dependences of displacement on energy offset. This is, generally, of no real advantage, inasmuch as the higher order terms are typically neither well known nor easily measured, and thus represent errors in the transformation of the beam.

Conditions on M_{56} and T_{566}. We now concatenate the linac and arc transforms to relate directly the injected phase space to the phase space at the wiggler. Under the conditions outlined above, the transformation is as follows.

$$\bar{z}(z) = z - M_{56}\left(\frac{V\left[\cos\left(\phi_0 - \frac{2\pi z}{\lambda}\right) - \cos\phi_0\right]}{E^{inj} + V\cos\phi_0}\right) - T_{566}\left(\frac{V\left[\cos\left(\phi_0 - \frac{2\pi z}{\lambda}\right) - \cos\phi_0\right]}{E^{inj} + V\cos\phi_0}\right)^2$$

$$\Delta\bar{E}(z) = V\left[\cos\left(\phi_0 - \frac{2\pi z}{\lambda}\right) - \cos\phi_0\right]$$

In our model, we assume a bunch of energy spread zero and bunch length L_{bunch}^{inj} injected with a phase offset ϕ_0 into a linac with total available RF voltage V. The resulting acceleration is to produce a bunch with energy spread no greater than ΔE^{FEL}, and, as the beam is relativistic, (and in order to minimize peak current through the acceleration cycle) the bunch length will remain essentially unchanged. Following acceleration, a magnetic transport system (referred to here as the "arc") is then assumed to transport the beam to the wiggler, and, while doing so, compress it to "zero" length (without affecting the energy spread). This will be accomplished, through second order in momentum offset, by proper choice of M_{56} and T_{566}.

Linac Transform. As above, displacement along the bunch is denoted by z; energy offset from design energy is denoted by ΔE. The dynamics of the phase space and RF during the acceleration cycle are schematically presented in Figure 2.

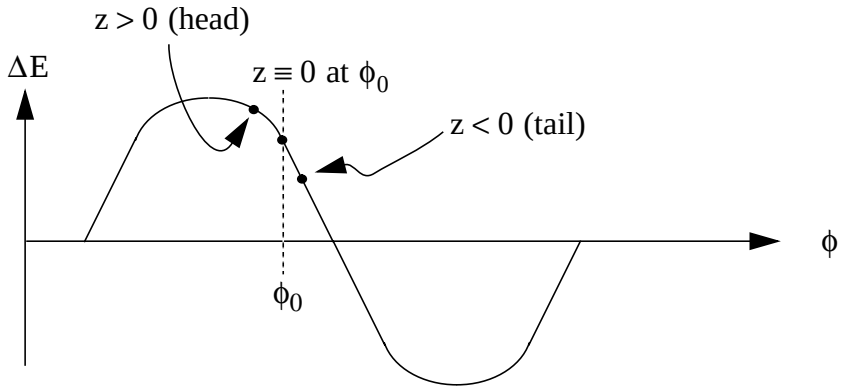

Figure 2: Schematic of RF dynamics in longitudinal phase space.

We note the head of the bunch ($z>0$) arrives earlier in phase than the bunch centroid, which is at a phase offset ϕ_0 relative to the crest of the accelerating waveform. This implies, in DIMAD notation, that $\delta l_{head}<0$. Similarly, the tail of the bunch ($z<0$) arrives later than the bunch centroid, implying $\delta l_{tail}>0$. The linac transformation is therefore as follows; here we have enforced the assumption that the initial momentum spread (ΔE^{inj}) is zero and taken advantage of the fact that for a straight-line baseline orbit (such as in a linac) M_{56} and T_{566} are zero.

$$\tilde{z}(z) = z$$

$$\Delta\tilde{E}(z) = \Delta E + V\left[\cos\left(\phi_0 - \frac{2\pi z}{\lambda}\right) - \cos\phi_0\right] = V\left[\cos\left(\phi_0 - \frac{2\pi z}{\lambda}\right) - \cos\phi_0\right]$$

parameters for this process fall into three categories - those associated with the injector, those specific to the FEL, and those related to the driver itself.

Injector Parameters. The key parameters for the injector are the injection energy, E^{inj}, the initial bunch length L^{inj}_{bunch}, the energy spread ΔE^{inj}, the bunch charge Q and charge distribution f(z). For the purposes of this discussion, we may treat the charge as constant through the acceleration process and assume the charge distribution is symmetric; peak current considerations then reduce to specification of the bunch length. The injection energy is injector specific, and is chosen to be at relativistic levels (at least several MeV) so that space charge effects may be ignored or minimized. We will assume the initial energy spread to be negligible; the dynamics of the driver accelerator are then dictated by the need to transform the long, essentially monoenergetic bunch into a high peak current (short) bunch of limited momentum spread.

FEL Parameters. The FEL is, in the context of this discussion, described by the required electron energy E^{FEL}, the maximum allowable energy spread at the wiggler ΔE^{FEL}, and the required peak current at the wiggler. As noted above, the peak current will be specified by the bunch length at the wiggler, L^{FEL}_{bunch}.

Driver Parameters. The driver accelerator is described by the total available RF voltage V, and ϕ_0, the phase offset of the bunch centroid from crest during acceleration. As we have indicated, the injection energy is relativistic so that any bunch compression during the acceleration cycle must be supplied through the use of magnetic bunch compression. The driver is therefore also described by linear and quadratic dependences of path length on relative momentum offset, which, in DIMAD notation, are referred to as M_{56} and T_{566}.

In the following investigation, we will ignore betatron/transverse focussing effects and concentrate on analysis of the constraints placed on the acceleration system and magnetic lattice (*via* M_{56} and T_{566}) by parameters specific to the injector and FEL. The system to be analytically treated is a simple accelerator and magnetic compression system that is constrained to map the low momentum spread injected phase space into the short bunch length phase space, as described above.

Longitudinal Dynamics of a Single-Pass Driver

We now address the coupling of FEL specific parameters to injector specific parameters though driver parameters. This is done by constructing a simple analytic model of longitudinal dynamics in a single pass (“one up, one down”) FEL driver, and investigating how the various parameters are related when the phase space manipulations described above and illustrated in Figure 1 are executed.

Analytic Modeling and Lattice Scaling Relations for FEL Driver Accelerators

D. Douglas, A. Hutton, C. Leemann, and *D. Neuffer*

Abstract

We analyze constraints on lattices for energy-recovering FEL driver accelerators. Parameters fundamental to the lattice of such accelerator systems are presented. An analytic model of longitudinal beam dynamics through the acceleration and energy recovery cycles of a single pass ("one up, one down") driver is developed. Relationships amongst parameters describing the injector, FEL, and accelerator lattice are established, and scaling laws derived.

Assumptions and Fundamental Parameters

The role of an FEL driver is to accelerate a low-energy, high charge-state electron bunch to some final energy E^{FEL} (required by FEL operation), while transforming the bunch to a state of high peak current and constraining the energy spread. This is to be accomplished while managing the electron beam transverse phase space in a manner consistent with FEL specifications. Typically, the injected bunch is configured to have modest momentum spread and to be fairly long (so as to minimize the effects of space charge and high peak current during acceleration). The acceleration and beam delivery process must therefore compress the bunch length, while keeping the relative momentum spread within limits dictated by FEL requirements.

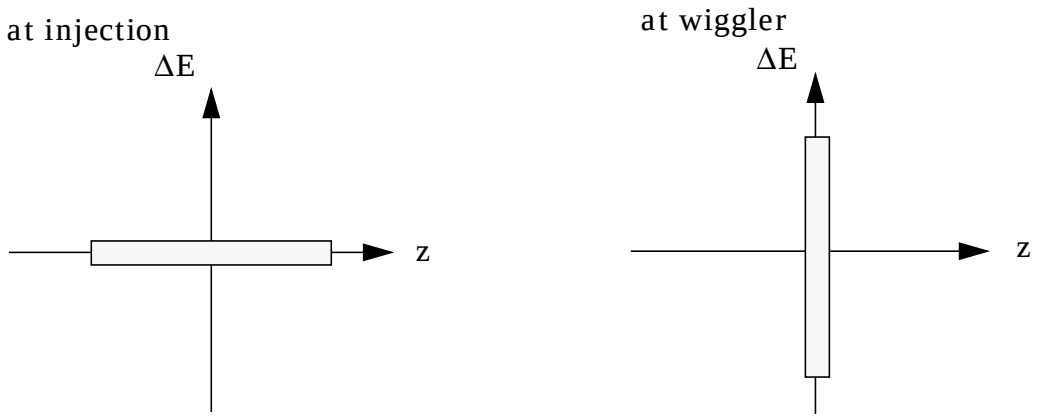

Figure 1: Idealized longitudinal phase space management provided by FEL driver.

An idealized scenario for this process is presented in Figure 1. Here, the horizontal, "z" axis is the longitudinal direction; the vertical axis is the energy offset from the reference orbit value. A "long, low-energy-spread" bunch is injected into a driver accelerator. Through the acceleration and beam handling process, this bunch is transformed into a "short, moderate-energy-spread" bunch at the wiggler. The key